SCIENCE CHINA
Information Sciences

• RESEARCH PAPER •

August 2024, Vol. 67, Iss. 8, 182202:1–182202:16
https://doi.org/10.1007/s11432-023-3980-0

State estimation for delayed switched positive systems: delayed radius approach

Weizhong CHEN[1,2], Zhongyang FEI[3,4*], Xudong ZHAO[3,4] & Zheng-Guang WU[5]

[1]*School of Electronics and Information, Xi'an Polytechnic University, Xi'an* 710048*, China;*
[2]*Research Institute of Intelligent Control and Systems, Harbin Institute of Technology, Harbin* 150001*, China;*
[3]*Key Laboratory of Intelligent Control and Optimization for Industrial Equipment of Ministry of Education, Dalian University of Technology, Dalian* 116024*, China;*
[4]*School of Control Science and Engineering, Dalian University of Technology, Dalian* 116024*, China;*
[5]*State Key Laboratory of Industrial Control Technology, Institute of Cyber-Systems and Control, Zhejiang University, Hangzhou* 310027*, China*

Received 10 September 2023/Revised 28 November 2023/Accepted 13 February 2024/Published online 4 July 2024

Abstract In this paper, an interval estimation scheme is developed for delayed switched positive systems (DSPS) with mode-dependent average dwell time switching. A lossless zonotopic estimation approach is proposed for the delayed intersection zonotope with the positive generator matrix. First, considering the existence of asynchronism between the system mode and the correction matrix mode, the mismatched intersection zonotope is constructed for DSPS to verify the consistency between the system model and outputs. Then, by utilizing the introduced radius definitions, the ℓ_∞ performance is addressed to optimize the size of delayed intersection zonotopes. Subsequently, we present a joint-design approach of switching signals and the mode-dependent correction matrix by constructing positive generator matrix-based delayed radius functions. Furthermore, guaranteed nonnegative state bounds are derived for the considered DSPS based on the proposed lossless zonotopic estimation criteria. Finally, detailed simulations are conducted to validate the feasibility and superiority of the developed methods.

Keywords delayed switched positive systems, interval estimation, asynchronous correction matrix, zonotopes, mode-dependent average dwell time

1 Introduction

Positive system is a specialized type of systems in which both the state and output remain positive given positive initial conditions. Due to the application of positive systems in economics, communication networks, etc., positive systems have garnered significant attention from researchers across various fields in recent decades [1–7]. Several positive systems and certain constrained switching rules constitute a switched positive system, which not only has positive characteristics but also exhibits switching features. Consequently, switched positive systems (SPS) have been utilized to describe or analyze some more complex systems, such as viral infection treatment, air conditioning systems, and so on [8–12]. Recently, many efforts have been increasingly devoted to investigating SPS [13–22]. For instance, by proving the existence of a copositive common functional for discrete-time SPS, some conditions guaranteeing the existence of state-dependent stabilizing switching signals were deduced by Fornasini and Valcher [14].

Note that state estimation and filtering for SPS have remained a research hotspot, yielding numerous reported findings [23–25]. By constructing a common co-positive Lyapunov functional and designing two positive sub-observers, Otsuka and Kakehi [23] addressed the interval estimation for continuous-time SPS under arbitrary switching. In [25], the stability and estimator design were solved for a class of SPS with average dwell time (ADT) switching by means of the reverse-timer-dependent co-positive Lyapunov functional method. Given the frequent influence of external interference or noise on real systems, the set-membership approach is deemed a more effective estimation method. It aims to calculate a set containing uncertain system states [23, 26, 27]. Furthermore, compared with ellipsoids and interval

* Corresponding author (email: zhongyangfei@dlut.edu.cn)

observer methods, the zonotopic estimation approach has several advantages, including simple calculation, easy implementation, and wrapping effect suppression [28–31]. In [29], based on the W_i radius, the authors paid attention to zonotopic state estimation for switched systems with bounded uncertainties.

In recent years, researchers have markedly focused on asynchronism, a typical phenomenon in switched systems [32,33]. For instance, the authors in [32] proposed a controller design scheme for asynchronously switched neutral systems with ADT signals. On the other hand, due to the limited signal transmission speed and memory effects of different units along the communication bus, time delay is ubiquitous in mechanical or engineering systems, which cannot be disregarded. Recently, some representative studies have been carried out for delayed SPS (DSPS) with asynchronism [34–36]. By employing the transition probability-based mode-dependent ADT (MDADT), the stability and stabilization were considered for asynchronously discrete-time DSPS [36]. However, research on state estimation for DSPS is still limited, highlighting the need for investigating such topics. Based on the clock-dependent copositive Lyapunov functional and dwell time switching strategy, positive observers for fuzzy DSPS with measurable and unmeasurable premise variables were respectively investigated by Li and Zhang [37]. To the best of the authors' knowledge, there are still no results covering on the interval estimation for DSPS, not even mention the asynchronism case. Here, our focus extends beyond solving this fundamental issue to devising a more efficient and straightforward method for estimating the upper and lower bounds of uncertain system states.

Based on the above discussions, this study aims to the zonotopic interval estimation for DSPS with matched and mismatched correction matrices. The uncertain states are contained in a guaranteed bound described by a delayed intersection zonotope. First, by introducing mode-dependent correction matrices, we deduce the over-approximation of the exact uncertain state set. Then, we establish an offline optimal method to improve the estimation accuracy for the considered DSPS utilizing constructed delayed radius functions. On the basis of the obtained ℓ_∞ analysis results, new conditions are developed to address the correction matrix design. Additionally, according to the zonotopic outer approximation, the positive upper and lower bounds are derived for the considered system. In order to corroborate the validity and advantages of the estimation schemes, numerical examples are given in Section 6.

Notations. $\mathbb{R}^n$ and $\mathcal{Z}$ denote the n-dimensional Euclidean space and the set of nonnegative integers, respectively. For any vector p and matrix $\mathcal{P}$, $\mathcal{P} > (\leqslant, \geqslant)0$ and $p > (\leqslant, \geqslant)0$ represent all entries of $\mathcal{P}$ and p are positive (nonpositive, nonnegative), respectively. $\boldsymbol{I}_n$ and $\mathbf{1}_n$ signify the n-dimensional identity matrix and the column vector with all its components as 1. For any matrix $\mathcal{P}$, $\boldsymbol{E}_{\downarrow\mathcal{P}}$ represents the matrix obtained by rearranging all columns of the matrix $\mathcal{P}$ with a rule of decreasing Euclidean norm, and $\mathrm{sum}(\mathcal{P}, 2)$ denotes the column vector formed by the sum of each row of the matrix $\mathcal{P}$. The vector 1-norm, weighted vector 1-norm, and vector ∞-norm are, respectively, defined as $\|p\|_1, \|p\|_Q$, and $\|p\|_\infty$, with $\|p\|_1 = \mathbf{1}^{\mathrm{T}}|p|$, $\|p\|_Q = \mathbf{1}^{\mathrm{T}}|Qp|$, Q is a positive definite matrix, and $\|p\|_\infty = \max_{1\leqslant i\leqslant n}|[p]_i|$, where $[\cdot]_i$ is the i-th component of the vector. For any $p(k) \in \mathbb{R}^n$, the ℓ_∞-norm $\|p\|_\infty = \sup_k \|p(k)\|_\infty$. A q-order zonotope $\mathbb{Z} = \langle c, M\rangle$ is a polytopic set, which can be described as $\mathbb{Z} = \{c + Mz : z \in \boldsymbol{B}^q\}$, where $\boldsymbol{B}^q = [-1, 1]^q \in \mathbb{R}^q$, M, and c represent the generator matrix and center of the zonotope $\mathbb{Z}$, respectively. For any matrix $H \in \mathbb{R}^{m\times n}$ and zonotopes $\mathbb{Z}_1 = \langle c_1, M_1\rangle, \mathbb{Z}_2 = \langle c_2, M_2\rangle, \mathbb{Z} = \langle c, M\rangle$ with $c_1, c_2, c \in \mathbb{R}^n, M_1, M_2, M \in \mathbb{R}^{n\times s}$, it holds that $\mathbb{Z}_1 \oplus \mathbb{Z}_2 = \langle c_1 + c_2, [M_1 \quad M_2]\rangle, H \odot \mathbb{Z} = \langle Hc, HM\rangle$.

2 Preliminaries

In the whole paper, we consider the following discrete-time DSPS:

$$\begin{cases} x(k+1) = A_{1\sigma(k)}x(k) + A_{2\sigma(k)}x(k - d(k)) + B_{\sigma(k)}u(k) + D_{\sigma(k)}\omega(k), \\ y(k) = C_{\sigma(k)}x(k) + E_{\sigma(k)}\omega(k),\ x(\upsilon) = \varepsilon(\upsilon),\ \upsilon = -d_2, \ldots, 0, \end{cases} \tag{1}$$

where $x(k) \in \mathbb{R}^{n_x}$ refers to the state vector; $u(k) \in \mathbb{R}^{n_u}$ is the input vector; $\omega(k) \in \mathbb{R}^{n_\omega}$ represents the bounded disturbance; $y(k) \in \mathbb{R}^{n_y}$ stands for the measured output vector. The piece-wise constant function $\sigma(k)$ is the system switching signal, the switching instant and switching sequence are, respectively, defined as $k_s, s \in \mathcal{Z}$, and $\{x(0); (p_0, k_0), (p_1, k_1), \ldots, (p_s, k_s), \ldots | p_s \in \mathcal{R}, s \in \mathcal{Z}\}$, with $\mathcal{R} = \{1, 2, \ldots, R\}$, $R > 1$ is the number of subsystems, and $k_0 = 0$. $d(k)$ is the time-varying delay satisfying $1 \leqslant d_1 \leqslant d(k) \leqslant d_2$, and $\varepsilon(\upsilon), \upsilon = -d_2, \ldots, 0$ is the initial condition. It is said that the switched system (1) is positive if $x(k) \geqslant 0$ and $y(k) \geqslant 0$ for any switching signal $\sigma(k)$ and any initial state $\varepsilon(\upsilon) \geqslant 0, \upsilon = -d_2, -d_2 + 1, \ldots, 0, u(k) \geqslant 0, \omega(k) \geqslant 0$.

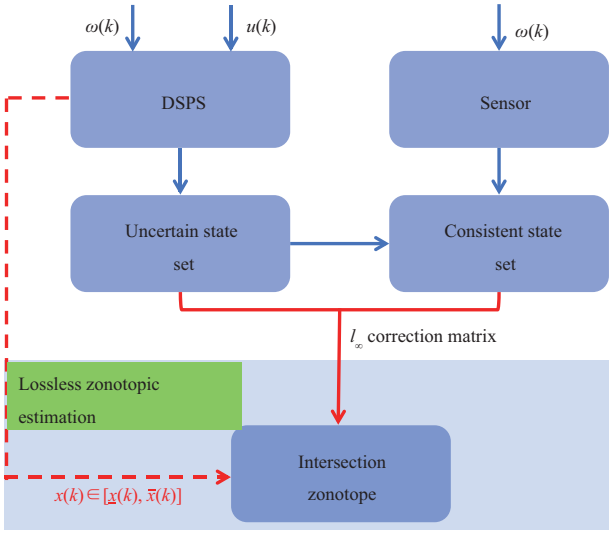

Figure 1 (Color online) Architecture of interval estimation for DSPS.

In this paper, system (1) is governed by MDADT switching, which is described as follows.

Definition 1 ([38]). The switching signal σ is said to be MDADT switching signal if there exist a real number τ_{ap} and an integer $\mathcal{N}_{0p} \geqslant 1$, such that $\mathcal{N}_{\sigma p}(k,K) \leqslant \mathcal{N}_{0p} + \frac{\mathcal{H}_p(k,K)}{\tau_{ap}}, p \in \mathcal{R}$, where $0 \leqslant k \leqslant K, \mathcal{N}_{\sigma p}(k,K)$ is the switching number during the time interval $[k,K)$ that the mode p is activated, $\mathcal{H}_p(k,K)$ is the overall running time of the subsystem p within $[k,K)$, and τ_{ap} is the MDADT.

Then, some necessary assumptions and lemmas are introduced for the follow-up work.

Assumption 1. The initial state $\varepsilon(\upsilon)$ and external perturbation $\omega(k)$ satisfy $\varepsilon(\upsilon) \in \mathbb{Z}_\upsilon = \langle c_\upsilon, M_\upsilon \rangle, M_\upsilon \geqslant 0, \upsilon = -d_2, -d_2+1, \ldots, 0 \leqslant \omega(k) \leqslant \bar{\omega}$.

Let $c_\omega = \bar{\omega}/2, M_\omega = \mathrm{diag}\{\bar{\omega}/2\}$. From Assumption 1, it yields that $\omega(k) \in \mathbb{Z}_\omega = \langle c_\omega, M_\omega \rangle$.

Lemma 1 ([3]). System (1) is positive if $A_{1i} \geqslant 0, A_{2i} \geqslant 0, B_i \geqslant 0, D_i \geqslant 0, C_i \geqslant 0, E_i \geqslant 0$, and $i \in \mathcal{R}$.

Lemma 2 ([26, 27]). For the zonotope $\mathbb{Z} = \langle c, M \rangle \subset \mathbb{R}^n, M \in \mathbb{R}^{n \times p}$, it holds that $\langle c, M \rangle = \mathbb{Z} \subseteq \langle c, M^g \rangle = \mathbb{Z}^g, n \leqslant g \leqslant p, \subseteq \langle c, rs(M^g) \rangle = \mathbf{Box}(\mathbb{Z}^g)$, where $\mathbb{Z}^g$ is the reduced order zonotope with the allowable maximum order g, and M^g is the generator matrix after reduction. $M^g = [\boldsymbol{E}_{\downarrow M}^{g-n} \quad \bar{M}]$, where $\boldsymbol{E}_{\downarrow M}^{g-n}$ is made of the first $g-n$ columns of the matrix $\boldsymbol{E}_{\downarrow M}$ and $\bar{M} = \mathrm{diag}\{\bar{m}_1, \ldots, \bar{m}_n\}, \bar{m}_i = \sum_{j=g-n+1}^{p} |\boldsymbol{E}_{\downarrow M_{i,j}}|, i = 1, \ldots, n$. $\mathbf{Box}(\mathbb{Z}^g)$ is the interval hull of the zonotope $\mathbb{Z}^g$, and $\mathbf{Box}(\mathbb{Z}^g) = \langle c, rs(M^g) \rangle$, where $rs(M^g) = \mathrm{diag}\{m_1^g, \ldots, m_n^g\}, m_i^g = \sum_{j=1}^{g} |M_{i,j}^g|, i = 1, \ldots, n$.

As depicted in Figure 1, suppose that $x(k-1)$ belongs to the zonotope $\tilde{\mathbb{Z}}_{k-1}$, the estimated set of the state $x(k)$ can be derived by the following three steps.

(1) Prediction: Based on system (1), we compute the uncertain state set $\tilde{\mathbb{Z}}_k$ to bound $x(k)$, where

$$\begin{aligned}\tilde{\mathbb{Z}}_k = &\big\{x(k) \in \mathbb{R}^{n_x} \mid \big(x(k) - B_{\sigma(k-1)}u(k-1)\big) \\ &\in A_{1\sigma(k-1)}\tilde{\mathbb{Z}}_{k-1} \oplus A_{2\sigma(k-1)}\tilde{\mathbb{Z}}_{k-1-d(k-1)} \oplus D_{\sigma(k-1)}\mathbb{Z}_\omega\big\}. \end{aligned} \tag{2}$$

(2) Measurement: Compute the consistent state set $\mathbb{Z}_{yk}$ using the measurement output y_k, where

$$\mathbb{Z}_{yk} = \big\{x(k) \in \mathbb{R}^{n_x} \mid (y(k) - C_{\sigma(k)}x(k)) \in E_{\sigma(k)}\mathbb{Z}_\omega\big\}. \tag{3}$$

(3) Correction: At time instant k, compute an intersection zonotope $\hat{\mathbb{Z}}_k$ as an outer bound of the exact uncertain state set $\mathbb{Z}_k$ that is the intersection between uncertain state set and consistent state set, where

$$\mathbb{Z}_k = \tilde{\mathbb{Z}}_k \cap \mathbb{Z}_{yk} \subseteq \hat{\mathbb{Z}}_k. \tag{4}$$

3 Interval estimation with matched correction matrix

In this section, an interval estimation strategy is proposed for DSPS by constructing proper delay-dependent radius functions and zonotopic outer approximation.

Algorithm 1 Lossless reduction operator for positive generator matrix-based zonotopes

Require: The positive generator matrix $M \in \mathbb{R}^{n\times p}$, the target order $g \geqslant n$;
Ensure: The reduced positive generator matrix $M^g = [\tilde{M} \quad \bar{M}]$;
1: **if** $g > p$ **then**
2: $M^g = M$;
3: **else**
4: Take the first $g-n$ columns of M to construct a new matrix $\tilde{M}$;
5: Create a diagonal matrix $\bar{M}$, where $\bar{M}(i,i) = \bar{g}_i, \bar{g}_i = \sum_{j=g-n+1}^{p} M_{i,j}, i = 1, 2, \ldots, n$;
6: **end if**

Lemma 3. For any p-order zonotope $\mathbb{Z} = \langle c, M\rangle \subset \mathbb{R}^n$ with positive generator matrix $M \in \mathbb{R}^{n\times p}$ and any matrix $Q \in \mathbb{R}^{n\times n} \geqslant 0$, different target orders for the zonotope $\mathbb{Z}$ do not affect the interval hull of the zonotope after the linear mapping by any positive matrix Q, i.e., $\mathbf{Box}(Q \odot \mathbb{Z}^n) = \mathbf{Box}(Q \odot \mathbb{Z}^s)$, where $n < s \leqslant p$.

Proof. According to Lemma 2, for the positive generator matrix $M \in \mathbb{R}^{n\times p}$ and different target orders, n, s $(n < s \leqslant p)$, easily, we have $M^n = \bar{M} = \mathrm{diag}\{\bar{m}_1, \ldots, \bar{m}_n\} \in \mathbb{R}^{n\times n}, \bar{m}_i = \sum_{j=1}^{p} |\boldsymbol{E}_{\downarrow M_{i,j}}|, i = 1, \ldots, n, M^s = [\boldsymbol{E}_{\downarrow M}^{s-n} \quad \bar{M}] \in \mathbb{R}^{n\times s}$, where $\boldsymbol{E}_{\downarrow M}^{s-n}$ is made of the first $s-n$ columns of the matrix $\boldsymbol{E}_{\downarrow M}$ and $\bar{M} = \mathrm{diag}\{\bar{m}_1, \ldots, \bar{m}_n\}$, $\bar{m}_i = \sum_{j=s-n+1}^{p} |\boldsymbol{E}_{\downarrow M_{i,j}}|, i = 1, \ldots, n$. From Lemma 2, note that $\boldsymbol{E}_{\downarrow M}$ in the reduction operator simply rearranges all the columns of the matrix M and does not affect the row sum of the matrix M. Meanwhile, because M is a positive generator matrix, the absolute value is redundant in the calculation of $\bar{M}$, and since $\bar{m}_i$ is also the calculation of the row sum, we can conclude that $\mathrm{sum}(M^n, 2) = \mathrm{sum}(M^s, 2)$. In addition, we can rewrite $\bar{M}$ in M^n and M^s as $\{\tilde{m}_1, \tilde{m}_2, \ldots, \tilde{m}_n\}$, where $\tilde{m}_i = [0; \cdots; \bar{m}_i; \cdots; 0] \in \mathbb{R}^n, i = 1, \ldots, n$. For any positive matrix $Q = [q_1; q_2; \cdots; q_n] \in \mathbb{R}^{n\times n}$, we have $Q \odot \mathbb{Z}^s = \langle Qc, QM^s\rangle, Q \odot \mathbb{Z}^n = \langle Qc, QM^n\rangle$, where

$$QM^s \in \mathbb{R}^{n\times s} = \begin{bmatrix} q_1\boldsymbol{E}_{\downarrow M}^1 & \cdots & q_1\boldsymbol{E}_{\downarrow M}^{s-n} & q_1\tilde{m}_1 & \cdots & q_1\tilde{m}_n \\ q_2\boldsymbol{E}_{\downarrow M}^1 & \cdots & q_2\boldsymbol{E}_{\downarrow M}^{s-n} & q_2\tilde{m}_1 & \cdots & q_2\tilde{m}_n \\ \vdots & \ddots & \vdots & \vdots & \ddots & \vdots \\ q_n\boldsymbol{E}_{\downarrow M}^1 & \cdots & q_n\boldsymbol{E}_{\downarrow M}^{s-n} & q_n\tilde{m}_1 & \cdots & q_n\tilde{m}_n \end{bmatrix}, \ QM^n \in \mathbb{R}^{n\times n} = \begin{bmatrix} q_1\tilde{m}_1 & \cdots & q_1\tilde{m}_n \\ q_2\tilde{m}_1 & \cdots & q_2\tilde{m}_n \\ \vdots & \ddots & \vdots \\ q_n\tilde{m}_1 & \cdots & q_n\tilde{m}_n \end{bmatrix}.$$

By combining with $\mathrm{sum}(M^n, 2) = \mathrm{sum}(M^s, 2)$, we can conclude that $rs(QM^s) = rs(QM^n)$. Thus, we derive that for different orders, $\mathbf{Box}(Q \odot \mathbb{Z}^n) = \mathbf{Box}(Q \odot \mathbb{Z}^s)$, where $n < s \leqslant p$.

Remark 1. The Minkowski sum of a zonotope increases its order [26, 27]. Apparently, the amount of calculation of the state zonotope will become increasingly larger as the number of the Minkowski sum increases. For this issue, the reduction operator is presented to limit the allowable maximum order of the zonotope [26]. In [26], the reduction operator gives priority to those more valuable generators (generators with greater Euclidean norm); therefore a lower target order can only get a rough boundary with less computational complexity. Thus, the choice of the target order should be combined with the actual situation to balance the calculation consumption and estimation accuracy, and we call the reduction operator in [26] the lossy reduction operator. In Lemma 3, we prove that for any zonotope with the positive generator matrix, under the linear mapping with any positive matrix, the order of the zonotope before the operation does not affect the interval hull of the new zonotope after the operation. Therefore, we can get a more accurate state estimation with the least amount of computation for positive generator matrix-based zonotopes (the target order is n_x). Here, we call this estimation lossless zonotopic estimation, and the lossless reduction operator is provided as Algorithm 1.

Definition 2. For the n-order intersection zonotope $\hat{\mathbb{Z}} = \langle \hat{c}, \hat{M}\rangle \subset \mathbb{R}^{n_x}, \hat{M} > 0$, the 1-norm-based radius and mode-dependent weighted radius are respectively defined as

$$\eta = \max_{b\in\boldsymbol{B}^n} \|\hat{M}b\|_1 = \|\hat{M}\mathbf{1}_n\|_1, \tag{5}$$

$$\zeta_i = \max_{b\in\boldsymbol{B}^n} \|\hat{M}b\|_{P_i} = \|\hat{M}\mathbf{1}_n\|_{P_i}, \tag{6}$$

where P_i is a positive matrix, $i \in \mathcal{R}$.

3.1 Delayed intersection zonotope with ℓ_∞ performance

In this subsection, the delayed intersection zonotope is given for the DSPS (1). Moreover, the boundedness and ℓ_∞ performance are discussed for the radius of the intersection zonotope.

Theorem 1. For the DSPS (1), $x(k) \in \hat{\mathbb{Z}}_k = \langle \hat{c}_k, \hat{M}_k \rangle$, output $y(k+1)$, state set $\mathbb{Z}_{yk+1}$, and suppose that there exist correction matrices $\Phi_{\sigma(k)}, \forall \sigma(k) \in \mathcal{R}$. Then, the delayed intersection zonotope $\hat{\mathbb{Z}}_{k+1}$, an outer bound of the exact uncertain state set $\mathbb{Z}_{k+1}$, can be devised as follows:

$$\hat{\mathbb{Z}}_{k+1} = \langle \hat{c}_{k+1}, \hat{M}_{k+1} \rangle, \tag{7}$$

where the center and generator matrix are, respectively, expressed as

$$\begin{aligned}\hat{c}_{k+1} =& (\boldsymbol{I}_{n_x} - \Phi_{\sigma(k)} C_{\sigma(k+1)}) A_{1\sigma(k)} \hat{c}_k + \Phi_{\sigma(k)} y(k+1) + (\boldsymbol{I}_{n_x} - \Phi_{\sigma(k)} C_{\sigma(k+1)}) A_{2\sigma(k)} \hat{c}_{k-d(k)} \\ & - (\Phi_{\sigma(k)} C_{\sigma(k+1)} D_{\sigma(k)} + \Phi_{\sigma(k)} E_{\sigma(k+1)} - D_{\sigma(k)}) c_\omega + (\boldsymbol{I}_{n_x} - \Phi_{\sigma(k)} C_{\sigma(k+1)}) B_{\sigma(k)} u(k), \qquad (8) \\ \hat{M}_{k+1} =& [(\boldsymbol{I}_{n_x} - \Phi_{\sigma(k)} C_{\sigma(k+1)}) A_{1\sigma(k)} \hat{M}_k \quad (\boldsymbol{I}_{n_x} - \Phi_{\sigma(k)} C_{\sigma(k+1)}) A_{2\sigma(k)} \hat{M}_{k-d(k)} \\ & (\boldsymbol{I}_{n_x} - \Phi_{\sigma(k)} C_{\sigma(k+1)}) D_{\sigma(k)} M_\omega \quad - \Phi_{\sigma(k)} E_{\sigma(k+1)} M_\omega]. \qquad (9)\end{aligned}$$

Furthermore, for the computed zonotope $\hat{\mathbb{Z}}$, given constants $0 < \alpha_p < 1, \mu_p > 1$, assume that there exist radius functions $\eta, \zeta_{\sigma(k)}$, and a scalar γ such that $\forall (p,q) \in \mathcal{R} \times \mathcal{R}, p \neq q$,

$$\zeta_p(k+1) \leqslant \alpha_p \zeta_p(k) + \Lambda(k), \tag{10}$$

$$\zeta_p(k_m) \leqslant \mu_p \zeta_q(k_m), \tag{11}$$

where $\Lambda(k) = -\eta(k) + \gamma^2 \eta_\omega(k), \eta_\omega(k) \leqslant \|\omega\|_\infty$. Then, for any MDADT switching signal satisfying

$$\tau_{ap} > \tau_{ap}^* = -\frac{\ln \mu_p}{\ln \alpha_p}, \tag{12}$$

the radius of the intersection zonotope $\hat{\mathbb{Z}}$ for the DSPS (1) is bounded with an ℓ_∞ performance γ.

Proof. Here, we first illustrate how to get the zonotope $\hat{\mathbb{Z}}_{k+1}$ by the three-step approach outlined in Section 2. For any $\hat{x}_{k+1} \in \tilde{\mathbb{Z}}_{k+1} \cap \mathbb{Z}_{yk+1}$, we have $\hat{x}_{k+1} \in \tilde{\mathbb{Z}}_{k+1}$ and $\hat{x}_{k+1} \in \mathbb{Z}_{yk+1}$. First, according to the Prediction step (2) and the system (1), one obtains that

$$\begin{aligned}\hat{x}_{k+1} =& A_{1\sigma(k)} \hat{c}_k + A_{2\sigma(k)} \hat{c}_{k-d(k)} + B_{\sigma(k)} u(k) + D_{\sigma(k)} c_\omega \\ & + [A_{1\sigma(k)} \hat{M}_k \quad A_{2\sigma(k)} \hat{M}_{k-d(k)} \quad D_{\sigma(k)} M_\omega] \boldsymbol{b}_1, \end{aligned} \tag{13}$$

where $\boldsymbol{b}_1 \in \boldsymbol{B}^{n_1+n_2+n_\omega}$ is a vector with an appropriate dimension. Then, from $\hat{x}_{k+1} \in \mathbb{Z}_{yk+1}$ and (1), for the Measurement step, there exists a suitable column vector $\boldsymbol{b}_2 \in \boldsymbol{B}^{n_\omega}$, such that

$$C_{\sigma(k+1)} \hat{x}_{k+1} = y(k+1) - E_{\sigma(k+1)} c_\omega - E_{\sigma(k+1)} M_\omega \boldsymbol{b}_2. \tag{14}$$

Moreover, by defining $\Pi_{k+1} = [A_{1\sigma(k)} \hat{M}_k \quad A_{2\sigma(k)} \hat{M}_{k-d(k)} \quad D_{\sigma(k)} M_\omega]$ and combining (13), (14), one has

$$\begin{aligned}C_{\sigma(k+1)} \Pi_{k+1} \boldsymbol{b}_1 =& - C_{\sigma(k+1)} A_{1\sigma(k)} \hat{c}_k - C_{\sigma(k+1)} A_{2\sigma(k)} \hat{c}_{k-d(k)} - C_{\sigma(k+1)} B_{\sigma(k)} u(k) \\ & - C_{\sigma(k+1)} D_{\sigma(k)} c_\omega + y(k+1) - E_{\sigma(k+1)} c_\omega - E_{\sigma(k+1)} M_\omega \boldsymbol{b}_2. \end{aligned} \tag{15}$$

On the other hand, for the Correction step, set $\Phi_{\sigma(k)} C_{\sigma(k+1)} \Pi_{k+1} \boldsymbol{b}_1$ as a correction term, where $\Phi_{\sigma(k)}$ is the correction matrix. Then, it yields from (13) that

$$\begin{aligned}\hat{x}_{k+1} =& A_{1\sigma(k)} \hat{c}_k + A_{2\sigma(k)} \hat{c}_{k-d(k)} + B_{\sigma(k)} u(k) + D_{\sigma(k)} c_\omega + (\boldsymbol{I}_{n_x} - \Phi_{\sigma(k)} C_{\sigma(k+1)}) \Pi_{k+1} \boldsymbol{b}_1 \\ & + \Phi_{\sigma(k)} C_{\sigma(k+1)} \Pi_{k+1} \boldsymbol{b}_1 \\ =& (\boldsymbol{I}_{n_x} - \Phi_{\sigma(k)} C_{\sigma(k+1)}) A_{1\sigma(k)} \hat{c}_k + \Phi_{\sigma(k)} y(k+1) + (\boldsymbol{I}_{n_x} - \Phi_{\sigma(k)} C_{\sigma(k+1)}) A_{2\sigma(k)} \hat{c}_{k-d(k)} \\ & - (\Phi_{\sigma(k)} C_{\sigma(k+1)} D_{\sigma(k)} + \Phi_{\sigma(k)} E_{\sigma(k+1)} - D_{\sigma(k)}) c_\omega + (\boldsymbol{I}_{n_x} - \Phi_{\sigma(k)} C_{\sigma(k+1)}) B_{\sigma(k)} u(k) \\ & + [(\boldsymbol{I}_{n_x} - \Phi_{\sigma(k)} C_{\sigma(k+1)}) A_{1\sigma(k)} \hat{M}_k \quad (\boldsymbol{I}_{n_x} - \Phi_{\sigma(k)} C_{\sigma(k+1)}) A_{2\sigma(k)} \hat{M}_{k-d(k)} \\ & (\boldsymbol{I}_{n_x} - \Phi_{\sigma(k)} C_{\sigma(k+1)}) D_{\sigma(k)} M_\omega \quad - \Phi_{\sigma(k)} E_{\sigma(k+1)} M_\omega] \boldsymbol{b}, \end{aligned}$$

where $\boldsymbol{b} = [\boldsymbol{b}_1; \boldsymbol{b}_2]$. Therefore, an intersection zonotope $\hat{\mathbb{Z}}_k$ can be gained for DSPS (1). Subsequently, the boundedness and the ℓ_∞ performance will be discussed for the radius of the delayed zonotope $\hat{\mathbb{Z}}$. Suppose that $\sigma(k_m) = p \neq q = \sigma(k_m - 1)$. According to conditions (10) and (11), it yields that $\zeta_{\sigma(k)}(k) \leqslant$

$\alpha_{\sigma(k)}^{k-k_m}\mu_{\sigma(k_m)}\zeta_{\sigma(k_m-1)}(k_m)+\sum_{\varrho=k_m}^{k-1}\alpha_{\sigma(k_m)}^{k-1-\varrho}\Lambda(\varrho)\leqslant\cdots\leqslant\alpha_{\sigma(k_m)}^{(k-k_m)}\cdots\alpha_{\sigma(k_0)}^{(k_1-k_0)}\mu_{\sigma(k_m)}\cdots\mu_{\sigma(k_1)}\zeta_{\sigma(k_0)}(k_0)+\cdots+\sum_{\varrho=k_m}^{k-1}\alpha_{\sigma(k_m)}^{k-1-\varrho}\Lambda(\varrho)$. Further, defining $\alpha_{\max}=\max_{p\in\mathcal{R}}\{\alpha_p\}$, by (12), we have

$$\zeta_{\sigma(k)}(k)\leqslant\Xi(\zeta_{\sigma(k_0)}(k_0))+\sum_{\varrho=k_0}^{k-1}\alpha_{\max}^{k-1-\varrho}\prod_{p=1}^{R}\mu_p^{\mathcal{N}_{\sigma p}(\varrho,k)}\Lambda(\varrho),\tag{16}$$

where $\Xi(\zeta_{\sigma(k_0)}(k_0))=\exp\{\sum_{p=1}^{R}\mathcal{H}_p(k_0,k)(\frac{1}{\tau_{ap}}\ln\mu_p+\ln\alpha_p)\}\prod_{p=1}^{R}\mu_p^{\mathcal{N}_{0p}}\zeta_{\sigma(k_0)}(k_0)$. Defining $\alpha_{\min}=\min_{p\in\mathcal{R}}\{\alpha_p\}$, from inequalities (12) and (16), one can deduce

$$\sum_{\varrho=k_0}^{k-1}\alpha_{\max}^{k-1-\varrho}\prod_{p=1}^{R}\mu_p^{\mathcal{N}_{0p}+\frac{\mathcal{H}_p(\varrho,k)}{\tau_{ap}}}\Lambda(\varrho)\leqslant\sum_{\varrho=k_0}^{k-1}\left(\frac{\alpha_{\max}}{\alpha_{\min}}\right)^{k-1-\varrho}\frac{1}{\alpha_{\min}}\prod_{p=1}^{R}\mu_p^{\mathcal{N}_{0p}}\Lambda(\varrho).\tag{17}$$

By combining (16) and (17), one further derives $\eta(k)\leqslant\Xi(\zeta_{\sigma(k_0)}(k_0))+\gamma^2\|\omega\|_\infty$. Thus, under the MDADT (12), the boundedness is satisfied for the radius of the zonotope $\hat{\mathbb{Z}}$ with the ℓ_∞ performance γ. The proof is completed.

3.2 Optimal correction matrix design

In this subsection, some solvable criteria are presented for the co-design of switching signals and the correction matrix based on Theorem 1.

Theorem 2. For given constants $0<\theta<1, 0<\alpha_p<1, \mu_p>1$, assume that there exist positive diagonal matrices $P_p\in\mathbb{R}^{n_x\times n_x}, Q_p\in\mathbb{R}^{n_x\times n_x}, p\in\mathcal{R}$ such that $\forall(p,q)\in\mathcal{R}\times\mathcal{R}$,

$$A_{1p}-\Phi_pC_qA_{1p}\geqslant 0,\ A_{2p}-\Phi_pC_qA_{2p}\geqslant 0,\ D_p-\Phi_pC_qD_p\geqslant 0,\ -\Phi_pE_q\geqslant 0,\tag{18}$$

$$\begin{cases}\mathbf{1}_{n_x}^{\mathrm{T}}\Psi_p\leqslant 0,\ \mathbf{1}_{n_x}^{\mathrm{T}}\Upsilon_p\leqslant 0,\ \mathbf{1}_{n_x}^{\mathrm{T}}\Omega_p-2n_\omega^{-1}\gamma^2(1-\theta)\mathbf{1}_{n_\omega}^{\mathrm{T}}\boldsymbol{I}_{n_\omega}\leqslant 0,\\ \mathbf{1}_{n_x}^{\mathrm{T}}\Theta_p-2n_\omega^{-1}\gamma^2\theta\mathbf{1}_{n_\omega}^{\mathrm{T}}\boldsymbol{I}_{n_\omega}\leqslant 0,\end{cases}\tag{19}$$

$$\mathbf{1}_{n_x}^{\mathrm{T}}P_p\leqslant\mu_p\mathbf{1}_{n_x}^{\mathrm{T}}P_q,\ \mathbf{1}_{n_x}^{\mathrm{T}}Q_p\leqslant\mu_p\mathbf{1}_{n_x}^{\mathrm{T}}Q_q,\ p\neq q,\tag{20}$$

where $\Psi_p=P_p(\boldsymbol{I}_{n_x}-\Phi_pC_p)A_{1p}-\alpha_pP_p+\boldsymbol{I}_{nx}+(d_2-d_1+2)Q_p, \Upsilon_p=P_p(\boldsymbol{I}_{n_x}-\Phi_pC_p)A_{2p}-\alpha_p^{d_2}Q_p, \Omega_p=P_p(\boldsymbol{I}_{n_x}-\Phi_pC_p)D_p, \Theta_p=-P_p\Phi_pE_p$. Then, for any MDADT switching signal satisfying (12), the radius of the intersection zonotope $\hat{\mathbb{Z}}$ for the DSPS (1) is bounded with an ℓ_∞ performance γ.

Proof. Defining $\hat{n}=n_1+n_2+2n_\omega$, for DSPS (1) and the delayed intersection zonotope $\hat{\mathbb{Z}}$, the mode- and delay-dependent weighted radius function can be constructed as follows:

$$\begin{aligned}\zeta_{\sigma(k+1)}(k+1)=&\max_{\hat{z}\in\boldsymbol{B}^{\hat{n}}}\|\hat{M}_{k+1}\hat{z}\|_{P_{\sigma(k+1)}}+\sum_{s=k+1-d(k+1)}^{k}\alpha_{\sigma(k+1)}^{k-s}\max_{z\in\boldsymbol{B}^n}\|\hat{M}_sz\|_{Q_{\sigma(k+1)}}\\&+\sum_{m=-d_2}^{-d_1}\sum_{s=k+m+1}^{k}\alpha_{\sigma(k+1)}^{k-s}\max_{z\in\boldsymbol{B}^n}\|\hat{M}_sz\|_{Q_{\sigma(k+1)}}.\end{aligned}\tag{21}$$

By the generator matrix (9) and the radius function (21), $\hat{z}$ is composed of suitable vectors z_1, z_2, b_1, and b_2, i.e., $\hat{z}=[z_1;z_2;b_1;b_2]$, where $z_1\in\boldsymbol{B}^{n_1}, z_2\in\boldsymbol{B}^{n_2}, b_1, b_2\in\boldsymbol{B}^{n_\omega}$. Setting $\eta_\omega(k)=\|\omega\|_\infty$, and according to Assumption 1, we can derive

$$\begin{aligned}\|\omega\|_\infty=&\sup_k\|\omega(k)\|_\infty=\max_{b\in\boldsymbol{B}^{n_\omega}}\|c_\omega+M_\omega b\|_\infty\\=&(1-\theta)\max_{b_1\in\boldsymbol{B}^{n_\omega}}\|c_\omega+M_\omega b_1\|_\infty+\theta\max_{b_2\in\boldsymbol{B}^{n_\omega}}\|c_\omega+M_\omega b_2\|_\infty,\end{aligned}\tag{22}$$

which is the worst-case condition of the disturbance ω. Then, for $\forall k\in[k_m,k_{m+1})$, by combining (21) with (22), the constraint (10) can be transformed as

$$\max_{\hat{z}\in\boldsymbol{B}^{\hat{n}}}\|\hat{M}_{k+1}\hat{z}\|_{P_p}-\alpha_p\max_{z_1\in\boldsymbol{B}^{n_1}}\|\hat{M}_kz_1\|_{P_p}+\max_{z_1\in\boldsymbol{B}^{n_1}}\|\hat{M}_kz_1\|_1+\max_{z_1\in\boldsymbol{B}^{n_1}}\|\hat{M}_kz_1\|_{Q_p}$$

$$
\begin{aligned}
&- \alpha_p^{d_2} \max_{z_2 \in \boldsymbol{B}^{n_2}} \|\hat{M}_{k-d(k)} z_2\|_{Q_p} + \sum_{s=k+1-d(k+1)}^{k-1} \alpha_p^{k-s} \max_{z \in \boldsymbol{B}^n} \|\hat{M}_s z\|_{Q_p} \\
&- \sum_{s=k+1-d(k)}^{k-1} \alpha_p^{k-s} \max_{z \in \boldsymbol{B}^n} \|\hat{M}_s z\|_{Q_p} + (d_2 - d_1 + 1) \max_{z_1 \in \boldsymbol{B}^{n_1}} \|\hat{M}_k z_1\|_{Q_p} \\
&- \sum_{s=k-d_2}^{k-d_1} \alpha_p^{k-s} \max_{z \in \boldsymbol{B}^n} \|\hat{M}_s z\|_{Q_p} - \gamma^2 (1-\theta) \max_{b_1 \in \boldsymbol{B}^{n_\omega}} \|c_\omega + M_\omega b_1\|_\infty \\
&- \gamma^2 \theta \max_{b_2 \in \boldsymbol{B}^{n_\omega}} \|c_\omega + M_\omega b_2\|_\infty \leqslant 0. \qquad (23)
\end{aligned}
$$

Further, it yields that

$$
\begin{aligned}
\sum_{s=k+1-d(k+1)}^{k-1} \alpha_p^{k-s} \max_{z \in \boldsymbol{B}^n} \|\hat{M}_s z\|_{Q_p} &\leqslant \sum_{s=k+1-d_2}^{k-1} \alpha_p^{k-s} \max_{z \in \boldsymbol{B}^n} \|\hat{M}_s z\|_{Q_p} \\
&= \sum_{s=k+1-d_2}^{k-d_1} \alpha_p^{k-s} \max_{z \in \boldsymbol{B}^n} \|\hat{M}_s z\|_{Q_p} + \sum_{s=k+1-d_1}^{k-1} \alpha_p^{k-s} \max_{z \in \boldsymbol{B}^n} \|\hat{M}_s z\|_{Q_p} \\
&< \sum_{s=k-d_2}^{k-d_1} \alpha_p^{k-s} \max_{z \in \boldsymbol{B}^n} \|\hat{M}_s z\|_{Q_p} + \sum_{s=k+1-d(k)}^{k-1} \alpha_p^{k-s} \max_{z \in \boldsymbol{B}^n} \|\hat{M}_s z\|_{Q_p}. \qquad (24)
\end{aligned}
$$

In terms of inequality (23), we can deduce the following condition:

$$
\gamma^2 (1-\theta) \max_{b_1 \in \boldsymbol{B}^{n_\omega}} \|c_\omega + M_\omega b_1\|_\infty \geqslant n_\omega^{-1} \gamma^2 (1-\theta) \max_{b_1 \in \boldsymbol{B}^{n_\omega}} \|c_\omega + M_\omega b_1\|_1. \qquad (25)
$$

Similar to (25), it holds that

$$
\gamma^2 \theta \max_{b_2 \in \boldsymbol{B}^{n_\omega}} \|c_\omega + M_\omega b_2\|_\infty \geqslant n_\omega^{-1} \gamma^2 \theta \max_{b_2 \in \boldsymbol{B}^{n_\omega}} \|c_\omega + M_\omega b_2\|_1. \qquad (26)
$$

As a result of (24)–(26), inequality (23) is realized if

$$
\begin{aligned}
&\max_{\hat{z} \in \boldsymbol{B}^{\hat{n}}} \|\hat{M}_{k+1} \hat{z}\|_{P_p} - \alpha_p \max_{z_1 \in \boldsymbol{B}^{n_1}} \|\hat{M}_k z_1\|_{P_p} + \max_{z_1 \in \boldsymbol{B}^{n_1}} \|\hat{M}_k z_1\|_1 + \max_{z_1 \in \boldsymbol{B}^{n_1}} \|\hat{M}_k z_1\|_{Q_p} \\
&\quad - \alpha_p^{d_2} \max_{z_2 \in \boldsymbol{B}^{n_2}} \|\hat{M}_{k-d(k)} z_2\|_{Q_p} + (d_2 - d_1 + 1) \max_{z_1 \in \boldsymbol{B}^{n_1}} \|\hat{M}_k z_1\|_{Q_p} \\
&\quad - n_\omega^{-1} \gamma^2 (1-\theta) \max_{b_1 \in \boldsymbol{B}^{n_\omega}} \|c_\omega + M_\omega b_1\|_1 - n_\omega^{-1} \gamma^2 \theta \max_{b_2 \in \boldsymbol{B}^{n_\omega}} \|c_\omega + M_\omega b_2\|_1 \leqslant 0. \qquad (27)
\end{aligned}
$$

According to Assumption 1 and (18), we deduce that the generator matrix (9) is positive. Furthermore, it follows from Definition 2 that

$$
\begin{aligned}
&\mathbf{1}_{n_x}^{\mathrm{T}} P_p \hat{M}_{k+1} \mathbf{1}_{\hat{n}} - \alpha_p \mathbf{1}_{n_x}^{\mathrm{T}} P_p \hat{M}_k \mathbf{1}_{n_1} + \mathbf{1}_{n_x}^{\mathrm{T}} \hat{M}_k \mathbf{1}_{n_1} + \mathbf{1}_{n_x}^{\mathrm{T}} Q_p \hat{M}_k \mathbf{1}_{n_1} - \alpha_p^{d_2} \mathbf{1}_{n_x}^{\mathrm{T}} Q_p \hat{M}_{k-d(k)} \mathbf{1}_{n_2} \\
&\quad + (d_2 - d_1 + 1) \mathbf{1}_{n_x}^{\mathrm{T}} Q_p \hat{M}_k \mathbf{1}_{n_1} - n_\omega^{-1} \gamma^2 (1-\theta) \mathbf{1}_{n_\omega}^{\mathrm{T}} c_\omega - n_\omega^{-1} \gamma^2 (1-\theta) \mathbf{1}_{n_\omega}^{\mathrm{T}} M_\omega \mathbf{1}_{b^1} \\
&\quad - n_\omega^{-1} \gamma^2 \theta \mathbf{1}_{n_\omega}^{\mathrm{T}} c_\omega - n_\omega^{-1} \gamma^2 \theta \mathbf{1}_{n_\omega}^{\mathrm{T}} M_\omega \mathbf{1}_{b^2} \leqslant 0, \qquad (28)
\end{aligned}
$$

which guarantees constraint (27), and $b^1 = b^2 = n_\omega$. Since $M_\omega = \mathrm{diag}\{c_\omega\}$, $\mathbf{1}_{n_\omega}^{\mathrm{T}} c_\omega = \mathbf{1}_{n_\omega}^{\mathrm{T}} M_\omega \mathbf{1}_{n_\omega}$. Then, Eq. (28) equals $\mathbf{1}_{n_x}^{\mathrm{T}} P_p \hat{M}_{k+1} \mathbf{1}_{\hat{n}} - \alpha_p \mathbf{1}_{n_x}^{\mathrm{T}} P_p \hat{M}_k \mathbf{1}_{n_1} + \mathbf{1}_{n_x}^{\mathrm{T}} (\boldsymbol{I}_{n_x} + Q_p) \hat{M}_k \mathbf{1}_{n_1} - \alpha_p^{d_2} \mathbf{1}_{n_x}^{\mathrm{T}} Q_p \hat{M}_{k-d(k)} \mathbf{1}_{n_2} + (d_2 - d_1 + 1) \mathbf{1}_{n_x}^{\mathrm{T}} Q_p \hat{M}_k \mathbf{1}_{n_1} - 2 n_\omega^{-1} \gamma^2 (1-\theta) \mathbf{1}_{n_\omega}^{\mathrm{T}} M_\omega \mathbf{1}_{b^1} - 2 n_\omega^{-1} \gamma^2 \theta \mathbf{1}_{n_\omega}^{\mathrm{T}} M_\omega \mathbf{1}_{b^2} \leqslant 0$. Replacing $\hat{M}_k$ with (9), it further yields that

$$
\mathbf{1}_{n_x}^{\mathrm{T}} \Psi_p \upsilon + \mathbf{1}_{n_x}^{\mathrm{T}} \Upsilon_p \epsilon + (\mathbf{1}_{n_x}^{\mathrm{T}} \Omega_p - 2 n_\omega^{-1} \gamma^2 (1-\theta) \mathbf{1}_{n_\omega}^{\mathrm{T}} \boldsymbol{I}_{n_\omega}) \phi + (\mathbf{1}_{n_x}^{\mathrm{T}} \Theta_q - 2 n_\omega^{-1} \gamma^2 \theta \mathbf{1}_{n_\omega}^{\mathrm{T}} \boldsymbol{I}_{n_\omega}) \varphi \leqslant 0, \qquad (29)
$$

where $\upsilon = \hat{M}_k \mathbf{1}_{n_1}, \epsilon = \hat{M}_{k-d(k)} \mathbf{1}_{n_2}, \phi = M_\omega \mathbf{1}_{b^1}, \varphi = M_\omega \mathbf{1}_{b^2}, \Psi_p = P_p (\boldsymbol{I}_{n_x} - \Phi_p C_p) A_{1p} - \alpha_p P_p + (d_2 - d_1 + 2) Q_p + \boldsymbol{I}_{n_x}, \Upsilon_p = P_p (\boldsymbol{I}_{n_x} - \Phi_p C_p) A_{2p} - \alpha_p^{d_2} Q_p, \Omega_p = P_p (\boldsymbol{I}_{n_x} - \Phi_p C_p) D_p, \Theta_p = -P_p \Phi_p E_p$. Therefore, if the condition (19) is true, Eq. (29) is established, which implies that inequality (10) holds. In addition, it is obvious that Eq. (11) is ensured by (20). Employing Theorem 1, thus, the radius of the zonotope $\hat{\mathbb{Z}}$ is bounded with an ℓ_∞ performance, which completes the proof.

Theorem 3. For given constants $0 < \theta < 1, 0 < \alpha_p < 1, \mu_p > 1$, assume that there exist arbitrary matrix $\hat{\Phi}_p \in \mathbb{R}^{n_x \times n_y}$ and positive diagonal matrices $P_p \in \mathbb{R}^{n_x \times n_x}, Q_p \in \mathbb{R}^{n_x \times n_x}, p \in \mathcal{R}$ such that $\forall (p,q) \in \mathcal{R} \times \mathcal{R}$,

$$P_p A_{1p} - \hat{\Phi}_p C_q A_{1p} \geqslant 0,\ P_p A_{2p} - \hat{\Phi}_p C_q A_{2p} \geqslant 0,\ P_p D_p - \hat{\Phi}_p C_q D_p \geqslant 0,\ -\hat{\Phi}_p E_q \geqslant 0, \tag{30}$$

$$\begin{cases} \mathbf{1}_{n_x}^{\mathrm{T}} \hat{\Psi}_p \leqslant 0, \mathbf{1}_{n_x}^{\mathrm{T}} \hat{\Upsilon}_p \leqslant 0, \mathbf{1}_{n_x}^{\mathrm{T}} \hat{\Omega}_p - 2 n_\omega^{-1} \gamma^2 (1-\theta) \mathbf{1}_{n_\omega}^{\mathrm{T}} \boldsymbol{I}_{n_\omega} \leqslant 0, \\ \mathbf{1}_{n_x}^{\mathrm{T}} \hat{\Theta}_p - 2 n_\omega^{-1} \gamma^2 \theta \mathbf{1}_{n_\omega}^{\mathrm{T}} \boldsymbol{I}_{n_\omega} \leqslant 0, \end{cases} \tag{31}$$

and Eq. (20) holds for $\forall (p,q) \in \mathcal{R} \times \mathcal{R}, p \neq q$ where $\hat{\Psi}_p = (P_p - \hat{\Phi}_p C_p) A_{1p} - \alpha_p P_p + (d_2 - d_1 + 2) Q_p + \boldsymbol{I}_{nx}, \hat{\Upsilon}_p = (P_p - \hat{\Phi}_p C_p) A_{2p} - \alpha_p^{d_2} Q_p, \hat{\Omega}_p = (P_p - \hat{\Phi}_p C_p) D_p, \hat{\Theta}_p = -\hat{\Phi}_p E_p$.

Then, for any MDADT switching signal satisfying (12), the radius of the intersection zonotope $\hat{\mathbb{Z}}$ for the DSPS (1) is bounded with an ℓ_∞ performance γ. Moreover, the optimal correction matrix Φ_p is designed by $\Phi_p = P_p^{-1} \hat{\Phi}_p, p \in \mathcal{R}$.

Proof. Since P_p is a positive diagonal matrix, we know that P_p^{-1} is also a positive diagonal matrix. By multiplying the left-hand side of the condition (30) by P_p^{-1}, obviously, we can get (18). On the other hand, Eq. (31) yields (19) by replacing $\hat{\Phi}_p$ with $P_p \Phi_p, p \in \mathcal{R}$. It completes the proof.

4 Interval estimation with mismatched correction matrix

In this section, the asynchronous interval estimation is addressed for DSPS (1). In the Correction step, we consider a more general case, the asynchronous correction matrix. Generally, if the system switches, due to external interference or communication faults, the transmission of system mode information may be delayed, thus affecting the timely update of the correction matrix mode. This will cause the correction matrix mode to lag behind the system mode over a period of time. Here, we set this time delay as $\delta(k)$, and assume $\delta_M = \max_{k \geqslant 0} \{\delta(k)\} \leqslant k_{m+1} - k_m$. Then, for $\sigma(k_m) = p \neq q = \sigma(k_m - 1), p, q \in \mathcal{R}$, the correction matrix Φ_q is operating during $[k_m, k_m + \delta(k_m))$ although the subsystem p is running. Further, the correction matrix Φ_p is active within the interval $[k_m + \delta(k_m), k_{m+1} + \delta(k_{m+1}))$. In this section, a correction-matrix-mode-dependent delayed radius function is constructed, which can better reflect the main characteristic of the asynchronous switching.

4.1 Delayed intersection zonotope with ℓ_∞ performance and asynchronism

This subsection considers the boundedness and ℓ_∞ performance for the DSPS (1) with the asynchronous correction matrix.

Theorem 4. For the DSPS (1), $x(k) \in \hat{\mathbb{Z}}_k = \langle \hat{c}_k, \hat{M}_k \rangle$, output $y(k+1)$, state set $\mathbb{Z}_{yk+1}$, suppose that there exist correction matrices $\Phi_{\sigma(k-\delta(k))}, \forall \sigma(k - \delta(k)) \in \mathcal{R}$. Then, the asynchronous intersection zonotope $\hat{\mathbb{Z}}_{k+1}$ can be calculated by

$$\hat{\mathbb{Z}}_{k+1} = \langle \hat{c}_{k+1}, \hat{M}_{k+1} \rangle, \tag{32}$$

with

$$\begin{aligned} \hat{c}_{k+1} = {} & (\boldsymbol{I}_{n_x} - \Phi_{\sigma(k-\delta(k))} C_{\sigma(k+1)}) A_{1\sigma(k)} \hat{c}_k + \Phi_{\sigma(k-\delta(k))} y(k+1) + (\boldsymbol{I}_{n_x} - \Phi_{\sigma(k-\delta(k))} C_{\sigma(k+1)}) A_{2\sigma(k)} \hat{c}_{k-d(k)} \\ & - (\Phi_{\sigma(k-\delta(k))} C_{\sigma(k+1)} D_{\sigma(k)} + \Phi_{\sigma(k-\delta(k))} E_{\sigma(k+1)} - D_{\sigma(k)}) c_\omega \\ & + (\boldsymbol{I}_{n_x} - \Phi_{\sigma(k-\delta(k))} C_{\sigma(k+1)}) B_{\sigma(k)} u(k), \end{aligned} \tag{33}$$

$$\begin{aligned} \hat{M}_{k+1} = {} & [(\boldsymbol{I}_{n_x} - \Phi_{\sigma(k-\delta(k))} C_{\sigma(k+1)}) A_{1\sigma(k)} \hat{M}_k \quad (\boldsymbol{I}_{n_x} - \Phi_{\sigma(k-\delta(k))} C_{\sigma(k+1)}) A_{2\sigma(k)} \hat{M}_{k-d(k)} \\ & (\boldsymbol{I}_{n_x} - \Phi_{\sigma(k-\delta(k))} C_{\sigma(k+1)}) D_{\sigma(k)} M_\omega \quad - \Phi_{\sigma(k-\delta(k))} E_{\sigma(k+1)} M_\omega]. \end{aligned} \tag{34}$$

Moreover, for the delayed zonotope $\hat{\mathbb{Z}}$ and given constants $0 < \alpha_p < 1, \beta_p > 1, \mu_p > 1, p \in \mathcal{R}$, assume that there exist radius functions $\eta, \zeta_{\sigma(k)}$, and a scalar γ such that $\sigma(k_m) = p \neq q = \sigma(k_m - 1), p, q \in \mathcal{R}$,

$$\forall k \in [k_m + \delta(k_m), k_{m+1}),\ \zeta_p(k+1) \leqslant \alpha_p \zeta_p(k) + \Lambda(k), \tag{35}$$

$$\forall k \in [k_m, k_m + \delta(k_m)),\ \zeta_q(k+1) \leqslant \beta_p \zeta_q(k) + \Lambda(k), \tag{36}$$

$$\zeta_p(k_m + \delta(k_m)) \leqslant \mu_p \zeta_q(k_m + \delta(k_m)). \tag{37}$$

Then, for any MDADT switching signal satisfying

$$\tau_{ap} > \tau_{ap}^{*} = -\frac{\delta_M \ln \varpi_p + \ln \mu_p}{\ln \alpha_p}, \tag{38}$$

with $\varpi_p = \beta_p/\alpha_p$, the radius of the asynchronous intersection zonotope $\hat{\mathbb{Z}}$ for the DSPS (1) is bounded with an ℓ_∞ performance γ.

Proof. Using the system model and the system output, we can derive (13)–(15). In the Correction step, the asynchronous correction matrix and asynchronous correction term are $\Phi_{\sigma(k-\delta(k))}$ and $\Phi_{\sigma(k-\delta(k))}C_{\sigma(k+1)}\Pi_{k+1}\boldsymbol{b}_1$, respectively. Then, obviously, according to the Prediction step (2) and (15),

$$\begin{aligned}\hat{x}_{k+1} =&(\boldsymbol{I}_{n_x} - \Phi_{\sigma(k-\delta(k))}C_{\sigma(k+1)})A_{1\sigma(k)}\hat{c}_k + \Phi_{\sigma(k-\delta(k))}y(k+1) + (\boldsymbol{I}_{n_x} - \Phi_{\sigma(k-\delta(k))}C_{\sigma(k+1)})A_{2\sigma(k)}\hat{c}_{k-d(k)}\\ &- (\Phi_{\sigma(k-\delta(k))}C_{\sigma(k+1)}D_{\sigma(k)} + \Phi_{\sigma(k-\delta(k))}E_{\sigma(k+1)} - D_{\sigma(k)})c_\omega + (\boldsymbol{I}_{n_x} - \Phi_{\sigma(k-\delta(k))}C_{\sigma(k+1)})B_{\sigma(k)}u(k)\\ &+ [(\boldsymbol{I}_{n_x} - \Phi_{\sigma(k-\delta(k))}C_{\sigma(k+1)})A_{1\sigma(k)}\hat{M}_k \quad (\boldsymbol{I}_{n_x} - \Phi_{\sigma(k-\delta(k))}C_{\sigma(k+1)})A_{2\sigma(k)}\hat{M}_{k-d(k)}\\ &(\boldsymbol{I}_{n_x} - \Phi_{\sigma(k-\delta(k))}C_{\sigma(k+1)})D_{\sigma(k)}M_\omega \quad - \Phi_{\sigma(k-\delta(k))}E_{\sigma(k+1)}M_\omega]\boldsymbol{b}\end{aligned}$$

holds, where the vector $\boldsymbol{b} = [\boldsymbol{b}_1; \boldsymbol{b}_2]$. Accordingly, the asynchronous intersection zonotope $\hat{\mathbb{Z}}_k$ is calculated.

In the following, we pay attention to the ℓ_∞ performance for the radius of the asynchronous zonotope $\hat{\mathbb{Z}}$. Assume that $\sigma(k_m) = p \neq q = \sigma(k_m - 1)$. In terms of conditions (35)–(37), for $\forall k \in [k_m + \delta(k_m), k_{m+1})$, one can deduce

$$\begin{aligned}\zeta_{\sigma(k_m)}(k) \leqslant&\alpha_{\sigma(k_m)}^{k-k_m}\cdots\alpha_{\sigma(k_0)}^{k_1-k_0}\varpi_{\sigma(k_m)}^{\delta_M}\cdots\varpi_{\sigma(k_0)}^{\delta_M}\mu_{\sigma(k_m)}\cdots\mu_{\sigma(k_0)}\zeta_{\sigma(k_0)}(k_0)\\ &-\cdots-\sum_{\varrho=k_m+\delta_M}^{k-1}\alpha_{\sigma(k_m)}^{k-1-\varrho}\Lambda(\varrho) - \mu_{\sigma(k_m)}\sum_{\varrho=k_m}^{k_m+\delta_M-1}\alpha_{\sigma(k_m)}^{k-1-\varrho}\varpi_{\sigma(k_m)}^{k_m+\delta_M-1-\varrho}\Lambda(\varrho).\end{aligned}$$

Furthermore, defining $\alpha_{\max} = \max_{p\in\mathcal{R}}\{\alpha_p\}$, $\varpi_{\max} = \max_{p\in\mathcal{R}}\{\varpi_p\}$, since $\varpi_{\sigma(k_m)}^{k_m+\delta_M-1-\varrho} \leqslant \varpi_{\sigma(k_m)}^{\delta_M-1}$ for $\varrho \in [k_m, k_m+\delta_M-1]$, we can obtain the following inequality:

$$\zeta_{\sigma(k)}(k) \leqslant \Xi(\zeta_{\sigma(k_0)}(k_0)) + \sum_{\varrho=k_0}^{k-1}\alpha_{\max}^{k-1-\varrho}\varpi_{\max}^{\delta_M-1}\prod_{p=1}^{R}(\mu_p\varpi_p^{\delta_M})^{\mathcal{N}_{\sigma p}(\varrho,k)}\Lambda(\varrho), \tag{39}$$

where $\Xi(\zeta_{\sigma(k_0)}(k_0)) = \exp\{\sum_{p=1}^{R}\mathcal{H}_p(k_0,k)[\frac{1}{\tau_{ap}}(\ln\mu_p + \ln\varpi_p^{\delta_M}) + \ln\alpha_p]\}\prod_{p=1}^{R}(\mu_p\varpi_p^{\delta_M})^{\mathcal{N}_{0p}}\zeta_{\sigma(k_0)}(k_0)$.

Similar to the proof of Theorem 1, we can further conclude that $\eta(k) \leqslant \Xi(\zeta_{\sigma(k_0)}(k_0)) + \gamma^2\|\omega\|_\infty$. Evidently, if the MDADT switching signal satisfies (38), $\Xi(\zeta_{\sigma(k_0)}(k_0))$ converges to zero as $k \to \infty$. Therefore, we conclude that the radius of the zonotope $\hat{\mathbb{Z}}$ for the DSPS (1) is bounded with the ℓ_∞ performance no greater than γ. It completes the proof.

4.2 Optimal asynchronous correction matrix design

Here, we will develop a joint-design approach for MDADT switching signals and asynchronous correction matrices.

Theorem 5. For given constants $0 < \theta < 1, 0 < \alpha_p < 1, \beta_p > 1, \mu_p > 1$, assume that there exist positive diagonal matrices $P_p \in \mathbb{R}^{n_x\times n_x}, Q_p \in \mathbb{R}^{n_x\times n_x}, p \in \mathcal{R}$ such that $\forall(p,q,r) \in \mathcal{R}\times\mathcal{R}\times\mathcal{R}$,

$$A_{1p} - \Phi_r C_q A_{1p} \geqslant 0,\ A_{2p} - \Phi_r C_q A_{2p} \geqslant 0,\ D_p - \Phi_r C_q D_p \geqslant 0,\ -\Phi_r E_q \geqslant 0, \tag{40}$$

$$\begin{cases}\mathbf{1}_{n_x}^{\mathrm{T}}\Psi_{pq} \leqslant 0, \mathbf{1}_{n_x}^{\mathrm{T}}\Upsilon_{pq} \leqslant 0, \mathbf{1}_{n_x}^{\mathrm{T}}\Omega_{pq} - 2n_\omega^{-1}\gamma^2(1-\theta)\mathbf{1}_{n_\omega}^{\mathrm{T}}\boldsymbol{I}_{n_\omega} \leqslant 0,\\ \mathbf{1}_{n_x}^{\mathrm{T}}\Theta_{pq} - 2n_\omega^{-1}\gamma^2\theta\mathbf{1}_{n_\omega}^{\mathrm{T}}\boldsymbol{I}_{n_\omega} \leqslant 0,\end{cases} \tag{41}$$

and Eqs. (19) and (20) hold, where $\Psi_{pq} = P_q(\boldsymbol{I}_{n_x} - \Phi_q C_p)A_{1p} - \beta_p P_q + \boldsymbol{I}_{n_x} + (d_2 - d_1 + 2)Q_q$, $\Upsilon_{pq} = P_q(\boldsymbol{I}_{n_x} - \Phi_q C_p)A_{2p} - \beta_p^{d_1}Q_q$, $\Omega_{pq} = P_q(\boldsymbol{I}_{n_x} - \Phi_q C_p)D_p$, $\Theta_{pq} = -P_q\Phi_q E_p$.

Then, for any MDADT switching signal satisfying (38), the radius of the asynchronous intersection zonotope $\hat{\mathbb{Z}}$ for the DSPS (1) is bounded with an ℓ_∞ performance γ.

Proof. For the DSPS (1) and the asynchronous intersection zonotope $\hat{\mathbb{Z}}$ (32), we choose correction-matrix-mode-dependent delayed radius functions for synchronous and asynchronous intervals, respectively. First, for the asynchronous interval $[k_m, k_m+\delta(k_m))$, we choose delayed radius functions:

$$\zeta_{\sigma(k_m-1)}(k+1) = \max_{\hat{z}\in\boldsymbol{B}^{\hat{n}}} \|\hat{M}_{k+1}\hat{z}\|_{P_{\sigma(k_m-1)}} + \sum_{s=k+1-d(k+1)}^{k} \beta_{\sigma(k_m)}^{k-s} \max_{z\in\boldsymbol{B}^n} \|\hat{M}_s z\|_{Q_{\sigma(k_m-1)}} + \sum_{m=-d_2}^{-d_1} \sum_{s=k+m+1}^{k} \beta_{\sigma(k_m)}^{k-s} \max_{z\in\boldsymbol{B}^n} \|\hat{M}_s z\|_{Q_{\sigma(k_m-1)}} \tag{42}$$

with $\hat{n} = n_1+n_2+2n_\omega$. Subsequently, for $\forall k \in [k_m, k_m+\delta(k_m))$, by combining (42) with (22), $\zeta_q(k+1) \leqslant \beta_p\zeta_q(k) + \Lambda(k)$ can be transformed as

$$\begin{aligned}
&\max_{\hat{z}\in\boldsymbol{B}^{\hat{n}}} \|\hat{M}_{k+1}\hat{z}\|_{P_q} - \beta_p \max_{z_1\in\boldsymbol{B}^{n_1}} \|\hat{M}_k z_1\|_{P_q} + \max_{z_1\in\boldsymbol{B}^{n_1}} \|\hat{M}_k z_1\|_1 + \max_{z_1\in\boldsymbol{B}^{n_1}} \|\hat{M}_k z_1\|_{Q_q} - \beta_p^{d_1} \max_{z_2\in\boldsymbol{B}^{n_2}} \|\hat{M}_{k-d(k)} z_2\|_{Q_q} \\
&+ \sum_{s=k+1-d(k+1)}^{k-1} \beta_p^{k-s} \max_{z\in\boldsymbol{B}^n} \|\hat{M}_s z\|_{Q_q} - \sum_{s=k+1-d(k)}^{k-1} \beta_p^{k-s} \max_{z\in\boldsymbol{B}^n} \|\hat{M}_s z\|_{Q_q} + (d_2-d_1+1) \max_{z_1\in\boldsymbol{B}^{n_1}} \|\hat{M}_k z_1\|_{Q_q} \\
&- \sum_{s=k-d_2}^{k-d_1} \beta_p^{k-s} \max_{z\in\boldsymbol{B}^n} \|\hat{M}_s z\|_{Q_q} - \gamma^2(1-\theta) \max_{b_1\in\boldsymbol{B}^{n_\omega}} \|c_\omega + M_\omega b_1\|_\infty - \gamma^2\theta \max_{b_2\in\boldsymbol{B}^{n_\omega}} \|c_\omega + M_\omega b_2\|_\infty \leqslant 0.
\end{aligned} \tag{43}$$

Then, based on inequalities (25) and (26), the inequality (43) holds if

$$\begin{aligned}
&\max_{\hat{z}\in\boldsymbol{B}^{\hat{n}}} \|\hat{M}_{k+1}\hat{z}\|_{P_q} - \beta_p \max_{z_1\in\boldsymbol{B}^{n_1}} \|\hat{M}_k z_1\|_{P_q} + \max_{z_1\in\boldsymbol{B}^{n_1}} \|\hat{M}_k z_1\|_1 + \max_{z_1\in\boldsymbol{B}^{n_1}} \|\hat{M}_k z_1\|_{Q_q} \\
&- \beta_p^{d_1} \max_{z_2\in\boldsymbol{B}^{n_2}} \|\hat{M}_{k-d(k)} z_2\|_{Q_q} + (d_2-d_1+1) \max_{z_1\in\boldsymbol{B}^{n_1}} \|\hat{M}_k z_1\|_{Q_q} - n_\omega^{-1}\gamma^2(1-\theta) \max_{b_1\in\boldsymbol{B}^{n_\omega}} \|c_\omega + M_\omega b_1\|_1 \\
&- n_\omega^{-1}\gamma^2\theta \max_{b_2\in\boldsymbol{B}^{n_\omega}} \|c_\omega + M_\omega b_2\|_1 \leqslant 0.
\end{aligned}$$

Here, considering the asynchronous correction matrix, the condition (40) can ensure the positivity of the generator matrix (34). Therefore, it yields

$$\begin{aligned}
&\mathbf{1}_{n_x}^{\mathrm{T}} P_q \hat{M}_{k+1} \mathbf{1}_{\hat{n}} - \beta_p \mathbf{1}_{n_x}^{\mathrm{T}} P_q \hat{M}_k \mathbf{1}_{n_1} + \mathbf{1}_{n_x}^{\mathrm{T}} \hat{M}_k \mathbf{1}_{n_1} + \mathbf{1}_{n_x}^{\mathrm{T}} Q_q \hat{M}_k \mathbf{1}_{n_1} - \beta_p^{d_1} \mathbf{1}_{n_x}^{\mathrm{T}} Q_q \hat{M}_{k-d(k)} \mathbf{1}_{n_2} \\
&+ (d_2-d_1+1)\mathbf{1}_{n_x}^{\mathrm{T}} Q_q \hat{M}_k \mathbf{1}_{n_1} - n_\omega^{-1}\gamma^2(1-\theta)\mathbf{1}_{n_\omega}^{\mathrm{T}} c_\omega - n_\omega^{-1}\gamma^2(1-\theta)\mathbf{1}_{n_\omega}^{\mathrm{T}} M_\omega \mathbf{1}_{b^1} \\
&- n_\omega^{-1}\gamma^2\theta \mathbf{1}_{n_\omega}^{\mathrm{T}} c_\omega - n_\omega^{-1}\gamma^2\theta \mathbf{1}_{n_\omega}^{\mathrm{T}} M_\omega \mathbf{1}_{b^2} \leqslant 0.
\end{aligned} \tag{44}$$

Obviously, the inequality (44) is true if $\mathbf{1}_{n_x}^{\mathrm{T}} P_q \hat{M}_{k+1} \mathbf{1}_{\hat{n}} - \beta_p \mathbf{1}_{n_x}^{\mathrm{T}} P_q \hat{M}_k \mathbf{1}_{n_1} + \mathbf{1}_{n_x}^{\mathrm{T}} (\boldsymbol{I}_{n_x} + Q_q) \hat{M}_k \mathbf{1}_{n_1} - \beta_p^{d_1} \mathbf{1}_{n_x}^{\mathrm{T}} Q_q \hat{M}_{k-d(k)} \mathbf{1}_{n_2} + (d_2-d_1+1)\mathbf{1}_{n_x}^{\mathrm{T}} Q_q \hat{M}_k \mathbf{1}_{n_1} - 2n_\omega^{-1}\gamma^2(1-\theta)\mathbf{1}_{n_\omega}^{\mathrm{T}} M_\omega \mathbf{1}_{b^1} - 2n_\omega^{-1}\gamma^2\theta \mathbf{1}_{n_\omega}^{\mathrm{T}} M_\omega \mathbf{1}_{b^2} \leqslant 0$. Thus, from (41), the inequality (36) is established. Next, considering the synchronous interval $[k_m + \delta(k_m), k_{m+1})$, we choose the radius function (21). According to the proof of Theorem 2, the inequality (35) is established by (19). In addition, it is obvious that Eq. (37) is established by the condition (20). Therefore, we conclude that the radius of the asynchronous intersection zonotope $\hat{\mathbb{Z}}$ is bounded and satisfies an ℓ_∞ performance no greater than γ, which completes the proof.

Theorem 6. For given constants $0 < \theta < 1, 0 < \alpha_p < 1, \beta_p > 1, \mu_p > 1$, assume that there exist arbitrary matrix $\hat{\Phi}_p \in \mathbb{R}^{n_x\times n_y}$ and positive diagonal matrices $P_p \in \mathbb{R}^{n_x\times n_x}, Q_p \in \mathbb{R}^{n_x\times n_x}, p \in \mathcal{R}$ such that $\forall (p,q,r) \in \mathcal{R}\times\mathcal{R}\times\mathcal{R}$,

$$P_r A_{1p} - \hat{\Phi}_r C_q A_{1p} \geqslant 0,\ P_r A_{2p} - \hat{\Phi}_r C_q A_{2p} \geqslant 0,\ P_r D_p - \hat{\Phi}_r C_q D_p \geqslant 0,\ -\hat{\Phi}_r E_q \geqslant 0, \tag{45}$$

$$\begin{cases}
\mathbf{1}_{n_x}^{\mathrm{T}} \hat{\Psi}_{pq} \leqslant 0, \mathbf{1}_{n_x}^{\mathrm{T}} \hat{\Upsilon}_{pq} \leqslant 0, \mathbf{1}_{n_x}^{\mathrm{T}} \hat{\Omega}_{pq} - 2n_\omega^{-1}\gamma^2(1-\theta)\mathbf{1}_{n_\omega}^{\mathrm{T}} \boldsymbol{I}_{n_\omega} \leqslant 0, \\
\mathbf{1}_{n_x}^{\mathrm{T}} \hat{\Theta}_{pq} - 2n_\omega^{-1}\gamma^2\theta \mathbf{1}_{n_\omega}^{\mathrm{T}} \boldsymbol{I}_{n_\omega} \leqslant 0,
\end{cases} \tag{46}$$

and Eqs. (20), (31) hold for $\forall (p,q) \in \mathcal{R}\times\mathcal{R}, p \neq q$ with $\hat{\Psi}_{pq} = (P_q - \hat{\Phi}_q C_p)A_{1p} - \beta_p P_q + (d_2-d_1+2)Q_q + \boldsymbol{I}_{n_x}, \hat{\Upsilon}_{pq} = (P_q - \hat{\Phi}_q C_p)A_{2p} - \beta_p^{d_1} Q_q, \hat{\Omega}_{pq} = (P_q - \hat{\Phi}_q C_p)D_p, \hat{\Theta}_{pq} = -\hat{\Phi}_q E_p$.

Then, for any MDADT switching signal satisfying (38), the radius of the asynchronous intersection zonotope $\hat{\mathbb{Z}}$ for the DSPS (1) is bounded with an ℓ_∞ performance γ. Furthermore, the asynchronous correction matrix Φ_p is designed by $\Phi_p = P_p^{-1}\hat{\Phi}_p, p \in \mathcal{R}$.

Proof. Similar to the proof of Theorem 3, we omit the detailed proof process here.

Algorithm 2 Interval estimation for DSPS

Require: $A_{1p}, A_{2p}, B_p, D_p, C_p, E_p, \bar{\omega}, \theta, \alpha_p, \mu_p, \beta_p, p \in \mathcal{R}, \mathbb{Z}_\upsilon, \upsilon = -d_2, \ldots, 0$;
Ensure: $[\underline{x}(k), \bar{x}(k)]$;
1: Solve conditions (20), (30), and (31) for the matched correction matrix case or (20), (31), (45), and (46) for the mismatched correction matrix case;
2: Return the ℓ_∞ correction matrix by Theorems 3 or 6;
3: **For** $k = 1 : K$ **do**
Based on the system (1) and derived correction matrices, calculate the center (8) or (33) and generator matrix (9) or (34);
Reduce the order of $\hat{M}_k$ by Algorithm 1;
Derive the state bounds by (47).
End

5 Interval estimation

In Sections 3 and 4, delayed intersection zonotopes with positive generator matrices are respectively deduced for synchronous and asynchronous state estimation schemes. Meanwhile, by constructing delayed radius functions, the optimal correction matrix Φ_p is obtained for every subsystem $p \in \mathcal{R}$. In addition, the positive generator matrix-based intersection zonotope can achieve lossless zonotopic estimation by Lemma 3. According to (7)–(9) and (32)–(34), time-varying intersection zonotopes are available for the DSPS (1) with matched and mismatched correction matrices, respectively, which completely contain uncertain system states. Then, according to Lemma 3 and Algorithm 2, we choose the target order $g = n_x$, and can derive the upper and lower bounds of the system state x as follows:

$$\begin{cases} \bar{x}(k) = \hat{c}_k + rs(\hat{M}_k^{n_x})\mathbf{1}_{n_x}, \\ \underline{x}(k) = \max\{0, \hat{c}_k - rs(\hat{M}_k^{n_x})\mathbf{1}_{n_x}\}. \end{cases} \tag{47}$$

6 Examples

Example 1. Consider a DSPS with the following parameters:

$$A_{11} = \begin{bmatrix} 0.2 & 0.4 \\ 0.1 & 0.3 \end{bmatrix}, A_{12} = \begin{bmatrix} 0.1 & 0.15 \\ 0.1 & 0.2 \end{bmatrix}, A_{21} = \begin{bmatrix} 0.02 & 0.05 \\ 0.02 & 0 \end{bmatrix}, A_{22} = \begin{bmatrix} 0 & 0.01 \\ 0.02 & 0.1 \end{bmatrix}, B_1 = \begin{bmatrix} 0.5 & 0.1 \\ 0.1 & 0.2 \end{bmatrix},$$
$$B_2 = \begin{bmatrix} 0.2 & 0.4 \\ 0.3 & 0.1 \end{bmatrix}, D_1 = \begin{bmatrix} 0.1 \\ 0.3 \end{bmatrix}, D_2 = \begin{bmatrix} 0.32 \\ 0.28 \end{bmatrix}, C_1 = \begin{bmatrix} 0.12 \\ 0.23 \end{bmatrix}^{\mathrm{T}}, C_2 = \begin{bmatrix} 0.2 \\ 0.15 \end{bmatrix}^{\mathrm{T}}, E_1 = 0.1, E_2 = 0.2.$$

Here, we choose $u(k) = 0.1\mathrm{rand}(1)$. In addition, according to Assumption 1, we assume the exogenous disturbance $\omega(k) = 0.1\mathrm{rand}(1)$ resulting in $\bar{\omega} = 0.1, c_\omega = M_\omega = 0.05$. Meanwhile, we select $\alpha_1 = 0.9, \alpha_2 = 0.95, \mu_1 = 1.3, \mu_2 = 1.2, \theta = 0.2, d_1 = 1, d_2 = 2, \gamma^2 = 5.5$.

First, we would demonstrate the effectiveness of our proposed interval estimation approach for DSPS with the matched correction matrix. By solving conditions (20), (30), and (31), the mode-dependent correction matrices $\Phi_p, p = 1, 2$ are calculated as $\Phi_1 = [-0.3535, -0.2780]^{\mathrm{T}}, \Phi_2 = [-0.5785, -0.1276]^{\mathrm{T}}$ with the MDADT $\tau_{a1}^* = 3, \tau_{a2}^* = 4$. In addition, we set the initial state zonotope $\mathbb{Z}_\upsilon = \langle [0.6, 0.6]^{\mathrm{T}}, \mathrm{diag}([0.3, 0.3]) \rangle$, $\upsilon = -2, -1, 0$, which implies that $\underline{x}(\upsilon) > 0$, i.e., the positive initial condition constraint. First, we choose the MDADT $\tau_{a1} = \tau_{a2} = 2$, and the switching signal is designed as displayed in Figure 2. Figure 3 shows the upper and lower bounds of states x_1 and x_2, where system states are completely wrapped by the estimated upper and lower bounds and the estimated lower bounds are nonnegative. These phenomena illustrate the correctness and effectiveness of our developed estimation method. Note that state bounds are depicted under different target orders ($g = 2, 15$) in Figure 3. It can be seen from Figure 3 that the order of the intersection zonotope does not affect the estimation accuracy, which verifies the applicability of the established Lemme 3 in Section 3. Furthermore, we discuss the effect of external disturbances on the estimation results. Here, we set $\omega(k) = 0.2\mathrm{rand}(1)$ and leave the rest of the parameters unchanged. It is worth mentioning that different magnitudes of external disturbances do not affect the co-design of the correction matrix and switching signals and the ℓ_∞ performance index γ. However, considering the relationship between the radius of the intersection zonotope and $\|\omega\|_\infty$, we know that larger magnitude

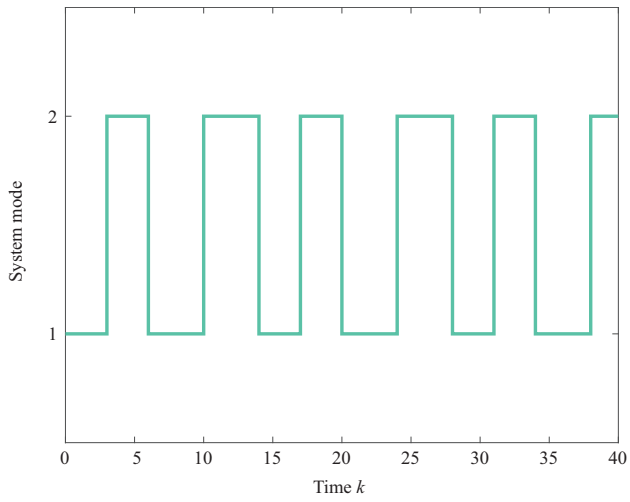

Figure 2 (Color online) Switching signal.

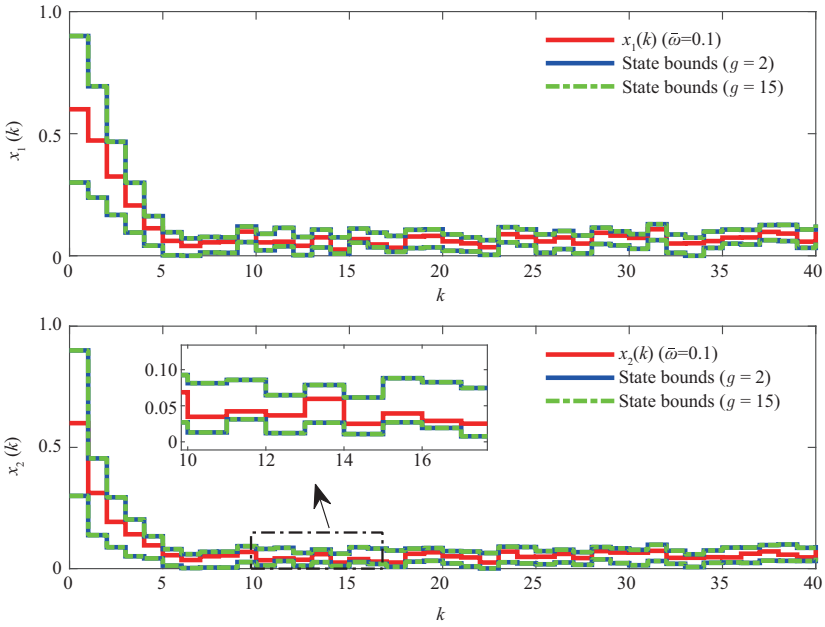

Figure 3 (Color online) State responses and boundaries of x.

disturbances will increase the radius of the intersection zonotope, which means the lower estimation accuracy, but the estimation schemes proposed in this paper have optimized the estimation accuracy as much as possible, including the lossless reduction operator and the ℓ_∞ performance of the radius.

Next, we emphasize that different orders do not affect the estimation results for the system state. Here, we take $x(5)$ for example, and the intersection state zonotopes for $g = 2, 15$ and their interval hulls are shown in Figure 4. From the left sub-graph, we can see that the shapes of zonotopes are different under different orders. However, according to Lemma 3, we know that the order of the zonotope before the reduction operation does not affect the interval hull of the new zonotope after the operation, which can be seen from the right sub-graphs in Figure 4. Therefore, our proposed estimation approach can achieve the lossless zonotopic estimation results, which also proves the superiority of our established state estimation scheme.

Example 2. In this example, we consider the asynchronism case. Borrowing from [20], we consider a DSPS with parameters

$$A_{11} = \begin{bmatrix} 0.3 & 0.2 \\ 0.1 & 0.3 \end{bmatrix}, \ A_{12} = \begin{bmatrix} 0.35 & 0.1 \\ 0.2 & 0.45 \end{bmatrix}, \ B_1 = \begin{bmatrix} 0.4 & 0.2 \\ 0.3 & 0.5 \end{bmatrix}, \ B_2 = \begin{bmatrix} 0.8 & 0.9 \\ 0.3 & 0.2 \end{bmatrix},$$

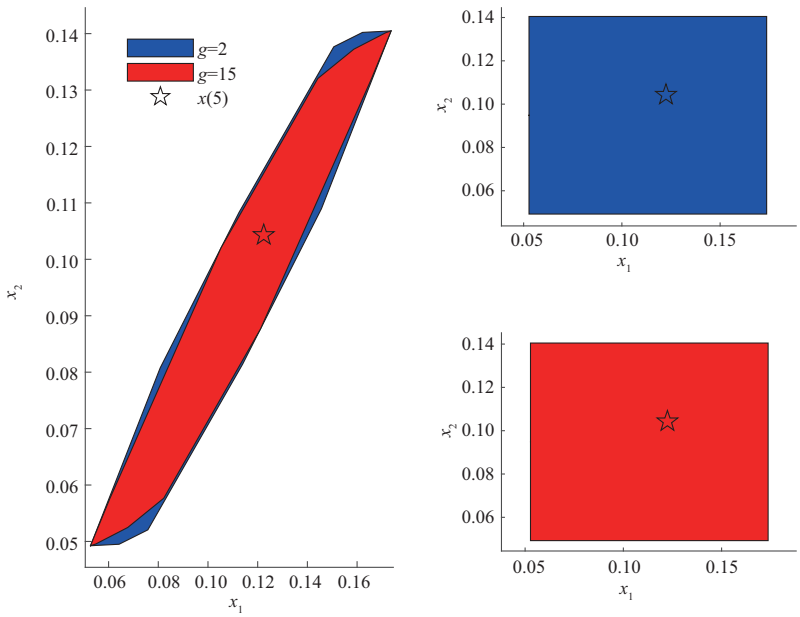

Figure 4 (Color online) Intersection zonotopes $\hat{\mathbb{Z}}_5^2$ and $\hat{\mathbb{Z}}_5^{15}$.

$$C_1 = \begin{bmatrix} 0.7 & 0 \\ 0.2 & 0.5 \end{bmatrix}, \ C_2 = \begin{bmatrix} 0.6 & 0.2 \\ 0.25 & 0.6 \end{bmatrix},$$

and we select

$$A_{21} = \begin{bmatrix} 0.02 & 0.1 \\ 0.02 & 0.15 \end{bmatrix}, \ A_{22} = \begin{bmatrix} 0.05 & 0 \\ 0.02 & 0.1 \end{bmatrix}, \ D_1 = \begin{bmatrix} 0.3 \\ 0.3 \end{bmatrix}, \ D_2 = \begin{bmatrix} 0.32 \\ 0.28 \end{bmatrix},$$

$$E_1 = \begin{bmatrix} 0.1 \\ 0 \end{bmatrix}, \ E_2 = \begin{bmatrix} 0.2 \\ 0.1 \end{bmatrix}.$$

First, we set $u(k) = 0.05\sin(k)\text{rand}(1) + 0.05$ and $\omega(k) = 0.16\text{rand}(1)$. Then, clearly, $\bar{\omega} = 0.16, c_\omega = M_\omega = 0.08$. Furthermore, we select $\alpha_1 = 0.9, \alpha_2 = 0.95, \mu_1 = 1.15, \mu_2 = 1.1, \theta = 0.2, d_1 = 1, d_2 = 2, \gamma = 2, \beta_1 = 1.02, \beta_1 = 1.01, \delta_M = 2$.

Here, our purpose is to achieve the interval estimation for DSPS with asynchronism by designing proper switching signals and a set of mode-dependent correction matrices. First, by Theorem 6, the MDADT switching signal and asynchronous correction matrices are computed as $\tau_{a1}^* = 3.7024, \tau_{a2}^* = 4.2461$, and

$$\Phi_1 = \begin{bmatrix} -0.0499 & -0.1116 \\ -0.7866 & 1.5153 \end{bmatrix}, \ \Phi_2 = \begin{bmatrix} -0.0571 & -0.1283 \\ -0.7814 & 1.4920 \end{bmatrix},$$

respectively. Next, let $\mathbb{Z}_\upsilon = \langle [0.5, 0.5]^{\mathrm{T}}, \text{diag}([0.5, 0.5]) \rangle, \upsilon = -2, -1, 0$ denote the initial state zonotope, which satisfies the positive initial condition constraint. Then, according to τ_{a1}^* and τ_{a2}^*, the MDADT switching signal is selected as shown in Figure 5. In terms of the obtained mode-dependent correction matrices and Theorem 4, the center and the generator matrix of the intersection zonotope can be obtained by (33) and (34), respectively. Further, by combining (47), we can acquire the lower and upper bounds of the uncertain system state, which are given in Figure 6 with the minimum target order 2. This demonstrates the validity and merits of our developed estimation method.

In the following, we will discuss the influence of the parameters α_p and β_p on the ℓ_∞ performance γ, where $p = 1, 2$. First, we set $\alpha_1 = 0.95, \alpha_2 = 0.98$, and $\beta_1 = \beta_2 = \beta$. By solving inequalities (20), (31), (45), and (46), the ℓ_∞ performance γ for different β are provided in detail in Table 1. From Table 1, we can conclude that a larger β will lead to a better ℓ_∞ performance. Then, we focus on the ℓ_∞ performance γ under different α. Choosing $\beta_1 = 1.05, \beta_2 = 1.08, \alpha_1 = \alpha_2 = \alpha$, the ℓ_∞ performance γ under different cases can be derived by Theorem 6, which are displayed in Table 2. It is clear that the bigger α is, the smaller γ is, that is, the better ℓ_∞ performance is.

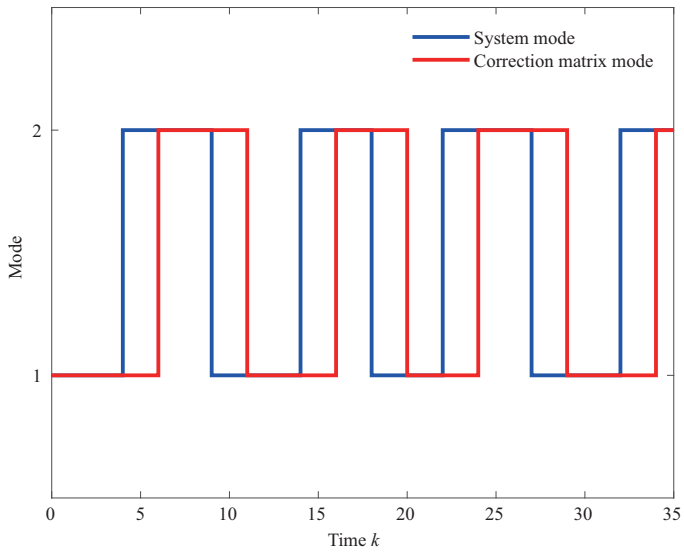

Figure 5 (Color online) Switching signal.

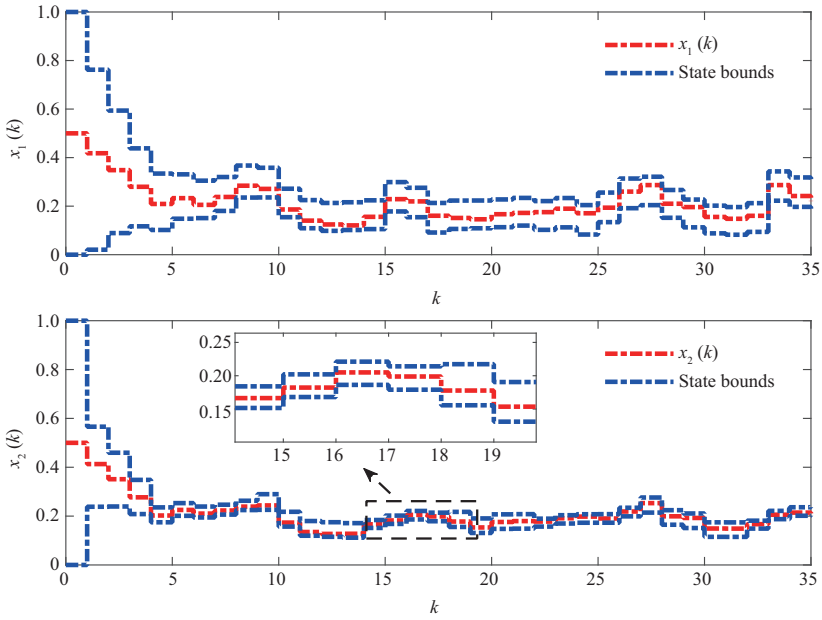

Figure 6 (Color online) State responses and boundaries of x.

Table 1 Optimal ℓ_∞ performance index γ with different β

	$\beta = 1.01$	$\beta = 1.05$	$\beta = 1.08$
γ	0.8713	0.8676	0.8651

Table 2 Optimal ℓ_∞ performance index γ with different α

	$\alpha = 0.75$	$\alpha = 0.85$	$\alpha = 0.95$
γ	2.7120	1.1784	0.8685

7 Conclusion

In this study, we constructed an interval estimation for a class of DSPS using a three-step interval estimation method. Our proposed estimation approach could obtain a guaranteed bound of uncertain system states, which contained the intersection between the uncertain state set and the consistent state set. First, a lemma was provided to prove the lossless estimation characteristic regarding the positive

generator matrix-based zonotope. Then, delayed intersection zonotopes were derived for matched and mismatched correction matrices, respectively. Furthermore, by constructing suitable delayed radius functions, a co-design approach was developed for switching signals and ℓ_∞ correction matrices. Finally, we calculated the time-varying estimation bounds to embrace the uncertain system states, which were certified by two illustrative examples.

Acknowledgements This work was supported in part by National Natural Science Foundation of China (Grant No. 62273069), Liaoning Revitalization Talents Program (Grant No. XLYC2203163), Natural Science Foundation of Shaanxi (Grant No. 2024JC-YBQN-0671), and PhD Research Startup Foundation of Xi'an Polytechnic University (Grant No. 310-107020646).

References

1 Deaecto G S, Geromel J C. $\mathcal{H}_2$ state feedback control design of continuous-time positive linear systems. IEEE Trans Automat Contr, 2017, 62: 5844–5849
2 Shen J, Lam J. Static output-feedback stabilization with optimal L_1-gain for positive linear systems. Automatica, 2016, 63: 248–253
3 Farina L, Rinaldi S. Positive Linear Systems: Theory and Applications. Hoboken: John Wiley & Sons, 2000. 50
4 Spagolla A, Morais C F, Oliveira R C L F, et al. Stabilization and $\mathcal{H}_2$ static output-feedback control of discrete-time positive linear systems. IEEE Trans Automat Contr, 2022, 67: 1446–1452
5 Knorn F, Mason O, Shorten R. On linear co-positive Lyapunov functions for sets of linear positive systems. Automatica, 2009, 45: 1943–1947
6 Wang X Z, Zhang H S, Xia J W, et al. Interval stability/stabilization of impulsive positive systems. Sci China Inf Sci, 2023, 66: 112203
7 Gao H, Li Z, Yu X, et al. Hierarchical multiobjective heuristic for PCB assembly optimization in a beam-head surface mounter. IEEE Trans Cybern, 2022, 52: 6911–6924
8 Hernandez-Vargas E, Colaneri P, Middleton R, et al. Discrete-time control for switched positive systems with application to mitigating viral escape. Intl J Robust Nonlinear, 2011, 21: 1093–1111
9 Jadbabaie A, Lin J, Morse A S. Coordination of groups of mobile autonomous agents using nearest neighbor rules. IEEE Trans Automat Contr, 2003, 48: 988–1001
10 Wang P, Zhao J. Almost output regulation for switched positive systems with different coordinates transformations and its application to a positive circuit model. IEEE Trans Circuits Syst I, 2019, 66: 3968–3977
11 Lin X, Xue J, Zheng E, et al. State-feedback stabilization for high-order output-constrained switched nonlinear systems. IEEE Trans Syst Man Cybern Syst, 2022, 52: 7401–7410
12 Gao H, An H, Lin W, et al. Trajectory tracking of variable centroid objects based on fusion of vision and force perception. IEEE Trans Cybern, 2023, 53: 7957–7965
13 Tian D D, Xia J W, Sun Y G, et al. Exponential stability analysis of switched positive nonlinear systems with impulsive effects via multiple max-separable Lyapunov functions. Sci China Inf Sci, 2023, 66: 169205
14 Fornasini E, Valcher M E. Stability and stabilizability criteria for discrete-time positive switched systems. IEEE Trans Automat Contr, 2012, 57: 1208–1221
15 Zheng J, Dong J G, Xie L. Stability of discrete-time positive switched linear systems with stable and marginally stable subsystems. Automatica, 2018, 91: 294–300
16 Guo Y, Wu Y, Gui W. Stability of discrete-time systems under restricted switching via logic dynamical generator and STP-based mergence of hybrid states. IEEE Trans Automat Contr, 2022, 67: 3472–3483
17 Xiang W, Lam J, Shen J. Stability analysis and L_1-gain characterization for switched positive systems under dwell-time constraint. Automatica, 2017, 85: 1–8
18 Ma R C, An S, Fu J. Dwell-time-based stabilization of switched positive systems with only unstable subsystems. Sci China Inf Sci, 2021, 64: 119205
19 Zheng Q, Xu S, Du B. Quantized guaranteed cost output feedback control for nonlinear networked control systems and its applications. IEEE Trans Fuzzy Syst, 2022, 30: 2402–2411
20 Ren Y, Sun G, Feng Z. Observer-based stabilization for switched positive system with mode-dependent average dwell time. ISA Trans, 2017, 70: 37–45
21 Ma L, Zhu F, Zhang J, et al. Leader-follower asymptotic consensus control of multiagent systems: an observer-based disturbance reconstruction approach. IEEE Trans Cybern, 2023, 53: 1311–1323
22 Yang G J, Hao F, Zhang L, et al. Exponential stability of discrete-time positive switched T-S fuzzy systems with all unstable subsystems. Sci China Inf Sci, 2021, 64: 159205
23 Otsuka N, Kakehi D. Interval switched positive observers for continuous-time switched positive systems under arbitrary switching. IFAC-PapersOnLine, 2019, 52: 250–255
24 Zheng Q, Xu S, Zhang Z. Nonfragile quantized H_∞ filtering for discrete-time switched T-S fuzzy systems with local nonlinear models. IEEE Trans Fuzzy Syst, 2020, 29: 1507–1517

25 Li Y, Zhang H. New results on stability analysis and estimator design for switched positive linear systems: a reverse-timer-dependent linear Co-positive Lyapunov function approach. IEEE Trans Circuits Syst II, 2021, 68: 697–701

26 Alamo T, Bravo J M, Camacho E F. Guaranteed state estimation by zonotopes. Automatica, 2005, 41: 1035–1043

27 Combastel C. Zonotopes and Kalman observers: gain optimality under distinct uncertainty paradigms and robust convergence. Automatica, 2015, 55: 265–273

28 Kühn W. Rigorously computed orbits of dynamical systems without the wrapping effect. Computing, 1998, 61: 47–67

29 Ifqir S, Puig V, Ichalal D, et al. Zonotopic set-membership estimation for switched systems based on W_i-Radius minimization: vehicle application. IFAC-PapersOnLine, 2020, 53: 7446–7451

30 Huang J, Che H, Raïssi T, et al. Functional interval observer for discrete-time switched descriptor systems. IEEE Trans Automat Contr, 2021, 67: 2497–2504

31 Liu H, Li Y, Han Q L, et al. Secure estimation, attack isolation, and reconstruction based on zonotopic unknown input observer. IEEE Trans Automat Contr, 2023, 68: 7312–7325

32 Wang Y E, Zhao J, Jiang B. Stabilization of a class of switched linear neutral systems under asynchronous switching. IEEE Trans Automat Contr, 2013, 58: 2114–2119

33 Qi Y, Yuan S, Niu B. Asynchronous control for switched T-S fuzzy systems subject to data injection attacks via adaptive event-triggering schemes. IEEE Trans Syst Man Cybern Syst, 2022, 52: 4658–4670

34 Xiang M, Xiang Z, Karimi H R. Asynchronous L_1 control of delayed switched positive systems with mode-dependent average dwell time. Inf Sci, 2014, 278: 703–714

35 Zhang M, Zhu Q. New criteria of input-to-state stability for nonlinear switched stochastic delayed systems with asynchronous switching. Syst Control Lett, 2019, 129: 43–50

36 Wang Y, Tang R, Su H, et al. Asynchronous control of switched discrete-time positive systems with delay. IEEE Trans Syst Man Cybern Syst, 2022, 52: 7193–7200

37 Li Y, Zhang H. Positive observer design for switched positive T-S fuzzy delayed systems with dwell time constraints. ISA Trans, 2020, 96: 37–50

38 Zhao X, Zhang L, Shi P, et al. Stability and stabilization of switched linear systems with mode-dependent average dwell time. IEEE Trans Automat Contr, 2011, 57: 1809–1815